DOI: 10.7860/JCDR/2026/78325.22714

Original Article

Dentistry Section

Estimating Osteogenic Potential of Rose Hip Seed Functionalised Hydroxyapatite Nanoparticles as a Bone Graft Substitute: An In-vitro Study

RADHIKA SRIMAGESH[1], RATNA PARAMESWARAN[2], SEERAB HUSAIN[3]

ABSTRACT

Introduction: Green synthesis is an environmentally friendly, non toxic method for formulating Hydroxyapatite Nanoparticles (HApNPs) and functionalising them using plant derivatives, such as Rose hip Seed extracts (Rh). Rose hip seeds have demonstrated osteogenic properties, making them ideal for synthesising a nanoparticle bone graft substitute capable of inducing bone formation.

Aim: To evaluate the osteogenic potential of Rose hip seed functionalised HApNPs.

Materials and Methods: The present study was an in-vitro investigation conducted in the Department of Orthodontics, Meenakshi Ammal Dental College and Hospital, Meenakshi Academy of Higher Education and Research (Deemed to be University), Chennai, Tamil Nadu, India from December 2022 to December 2024. synthesis of Rose hip Seed Extract-functionalised HApNPs (RhHApNPs) was carried out. The nanoparticles were subjected to physical characterisation, including HApNPs Field Emission Scanning Electron Microscopy (FESEM) analysis Energy-dispersive X-ray (EDX) analysis X-ray Diffraction (XRD) analysis Attenuated Total Reflection Fourier Transform Infrared Spectroscopy (ATR-FTIR) analysis. Biological characterisation involved a haemolytic test, while chemical characterisation included the Calcium Mineralisation Assay, Alkaline Phosphatase (ALP) activity test, and collagen estimation test. The outcomes of these tests were represented graphically using Origin software.

Results: The FESEM analysis revealed elongated, hexagonal, and spherical-shaped RhHApNPs, with a particle size range of 10-50 nm. EDX analysis demonstrated characteristic elemental peaks for Ca, P, O, and C in RhHApNPs. The XRD test indicated 55.6% crystallinity. ATR-FTIR analysis identified peaks of $PO4^{3-}$, along with the presence of other functional groups. The blood compatibility test results showed that the rate of haemolysis was below 5%, indicating good blood compatibility. RhHApNPs exhibited greater mineralisation density compared to non RhHApNPs, evidenced by higher Optical Density (OD). The ALP Activity test showed increased levels of ALP expression in RhHApNPs compared to non functionalised counterparts. The collagen estimation assay revealed collagen formation over NIH 3T3 cell line culture.

Conclusion: The newly synthesised RhHApNPs were elongated, hexagonal, and spherical, with a size range of 10-50 nm, demonstrating a Ca/P weight % of 1.99 and a crystallinity of 55.6%. The RhHApNPs also exhibited good haemocompatibility and increased osteogenic activity when compared to non functionalised HApNPs.

Keywords: Bone substitute, osseoinductive, Osteogenesis

INTRODUCTION

Bone regeneration in contemporary methods involves the use of biomaterials that are bioinert, biotolerant, bioresorbable, and biocompatible in nature [1]. Hydroxyapatite (HAp) constitutes the main mineral component of bone and teeth. The stoichiometric data of hydroxyapatite reveals a calcium to phosphorus ratio of 1.67 (by weight), which forms the least soluble and most stable form of calcium phosphate in nature [2]. They are high-order structured materials that act as an advancing front in bone regeneration [3]. Since, HAp is bioactive, it reacts with the bone tissues in immediate contact even before interacting with body fluids, thereby forming a chemical bond with the bone [4]. This phenomenon increases the stability and mechanical loading capacity of the bony scaffold. Since HAp materials are bioresorbable, they are eventually substituted by bone, mimicking fracture healing [5].

Nanoparticles are ultrafine substances used as vehicles to deliver an increased concentration of drugs to various parts of the body for sustained release [6]. HAp Nanoparticles (HApNPs) possess osteoconductive properties [7]. Several green synthesis methods have been employed for the formulation of HApNPs, utilising both plant and animal sources [8,9]. Plant phytochemicals play a dual role by acting as reducing and stabilising agents in the synthesis of nanoparticles, and the incorporation of these biomolecules enhances the nanoparticles' functional properties. However, most formulations of HApNPs do not possess the osteoinductive properties necessary to initiate osteogenic activity. Some plant extracts, such as rose hip seeds, Terminalia arjuna, Cissus quadrangularis, and Piper sarmentosum, have been shown to possess osteogenic potential [10-13].

The rose hip plant belongs to the Rosa genus in the Rosaceae family and is part of the ancient ancestral "Protocaninnae" group. It was first employed for medicinal use by Pliny the Elder (23-79 BC). R. canina has been used for its medicinal benefits due to its health-promoting components, such as flavonoids, fatty acids, carotenoids, antioxidants, anti-inflammatory agents, and high levels of vitamins (C, B, E) [14]. Owing to the presence of bioactive compounds, rose hip aids in synergistic antioxidant and bone formation properties. The antioxidant properties of rose hip positively affect the prevention of bone loss associated with oxidative stress [15].

Hydroxyapatite acts as a scaffolding material due to its osteoconductive properties. Previous studies have shown that rose hip seed extracts possess osseoinductive properties capable of promoting osteoblastic effects in samples [16,17]. The present study focuses on the formulation of HApNPs from plant sources (rose

hip seeds) and evaluating their physical, chemical, and biological properties through in-vitro experiments.

MATERIALS AND METHODS

The present study was an in-vitro investigation conducted in the Department of Orthodontics, at Meenakshi Ammal Dental College and Hospital, Meenakshi Academy of Higher Education and Research (Deemed to be University), Chennai, Tamil Nadu, India, from December 2022 to December 2024, adhering to Institutional Ethical Committee (IEC) protocol number MADC/IEC- IV/127/2022

Study Procedure

Preparation and Synthesis of HApNPs: The synthesis of Rose Hip Hydroxyapatite Nanoparticles (RhHApNPs) involved a multi-step procedure designed to ensure proper nucleation, particle stability, and functionalisation. Two hundred grams of rose hip seeds were thoroughly washed under running water and shade-dried for 48 hours at room temperature [Table/Fig-1a]. Once dried, the seeds were finely ground using a mortar and pestle [Table/Fig-1b]. One gram of the powder was mixed with 100 mL of distilled water [Table/Fig-1c]. This solution was placed in an orbital shaker for 24 hours [Table/Fig-1d] and then filtered.

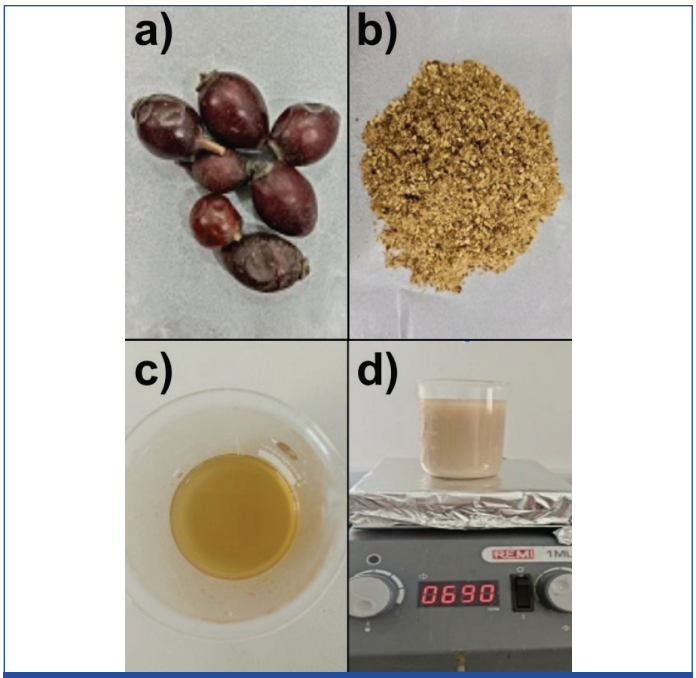

[Table/Fig-1]: (a) Dried Rose hip seeds; (b) Ground Rose hip seeds; (c) Rose hip seed extract; (d) RhHApNps solution in an orbital shaker.

A 0.6 M Orthophosphoric acid (H_3PO_4) solution was prepared and reacted with 1 M calcium chloride to initiate the formation of HAp, mimicking biomimetic mineralisation. The addition of rose hip extract introduced natural phytochemicals acting as both reducing and stabilising agents. The mixture was agitated for an additional hour to enhance the binding and interaction of bioactive compounds. Ammonium Hydroxide (NH_4OH) was gradually added to adjust the pH to 10, an optimal value for HAp precipitation, as alkaline conditions favour the nucleation and crystallisation of hydroxyapatite. The solution was agitated for a further three hours to promote the formation of a stable colloidal suspension.

To remove excess moisture and initiate particle formation, the solution was dried at 45°C for 24 hours, followed by heating at 125°C for 12 hours to eliminate residual solvents and encourage initial structural consolidation. The dried mass was then calcined at 800°C for three hours in a muffle furnace. This temperature was specifically chosen to improve the crystallinity of HAp while removing any organic residues from the rose hip extract without compromising its core structure. The final product, a yellowish porous powder of RhHApNPs, was then subjected to physical characterisation [18-20].

I. Physical characterisation:

a. Field Emission Scanning Electron Microscopy (FESEM) analysis: The SEM imaging of rose hip seed extract functionalised HAp was performed using FESEM JSM-IT 800 Schottky FESEM, JEOL Ltd. The SEM images were recorded with a magnification of FOV: 9.85 x 7.38 µm, 1.00 KV, WD 2.6 mm.

b. Energy-Dispersive X-Ray (EDX) analysis: The EDX analysis was performed for the RhHAp to determine the elemental composition of each material using EDX Spectroscopy Systems, Oxford Instruments.

c. XRD (X-ray Diffraction) analysis: RhHAp powder was subjected to an X-ray light beam using an X-ray diffractor (Bruker D8 - Discover). The diffractometer employed Cu K-α radiation with a wavelength of 0.15418 nm to determine the hydroxyapatite structure and crystallinity. The percentage of crystallinity of the hydroxyapatite was calculated using the following formula [21]:

% Crystallinity = (Area of the crystalline peak / Area of the amorphous and crystalline peaks) × 100

d. Attenuated total reflection - Fourier Transform Infrared (ATR-FTIR) spectroscopy analysis: The-FTIR was performed at room temperature with a resolution of 4 cm^{-1} and 32 scans per measurement. The software utilised was OPUS (Bruker) for data acquisition and analysis, after performing baseline correction. Origin 2015 (OriginLab) was employed for data fitting and plotting [22].

II. Biological Characterisation

Blood compatibility: The biocompatibility of the prepared RhHAp was assessed to determine haemolytic activity. The observed groups included Positive Control (PC) - Water, Negative Control (NC) - Saline, 10 µg/mL of RhHAp suspension, and 25 mg/mL of RhHAp. This assessment was performed to observe the material's reaction with bodily fluids, along with stability and biocompatibility.

One mg of RhHAp was diluted with 1.25 mL of sterile saline solution. Four mL of blood was then diluted with 5 mL of sterile saline solution. One mg/dL of diluted RhHAp sterile saline solution was mixed with 20 µL of diluted blood and incubated at 37°C for 30 minutes. The set-up was then left for 24-48 hours to determine the amount of haemolysis occurring in the Red Blood Cells (RBCs). The haemolytic percentage of the samples was calculated and plotted using the following formula [23].

$$\% \text{ Haemolysis} = \frac{\text{OD value of the test sample - OD values of the negative control}}{\text{OD values of the positive control - OD values of the negative control}} \times 100$$

III. Chemical characterisation:

a. Calcium mineralisation assay: The Alizarin Red Staining (ARS) was performed to identify mineralisation nodule formation using 100 mg of untreated cells (control), normal HAp, and RhHAp. A total of 40 mL of distilled water was added to 500 mg of Alizarin Red stain, and the pH was adjusted to 4.1. The solution was then diluted to 50 mL with distilled water to achieve a final concentration of 40 mM. Cells from each well of the culture medium were gently washed three times with 1X Phosphate Buffered Solution (PBS). The cells were fixed in 4% formaldehyde for 15 minutes at room temperature. After fixation, they were removed from the fixative and washed three times with distilled water. Then, 1 mL of 40 mM ARS was added per well. This set-up was incubated at room temperature for 20-30 minutes on an orbital shaker. The dye was removed by washing the cells five times with distilled water. At this stage, the cells were inspected for staining under phase-contrast microscopy. The plate was then tilted for two minutes to facilitate the removal of excess water, and the plates were stored at -20°C before dye extraction [24].

b. Alkaline Phosphatase (ALP) activity:

i. Preparation of 5-Bromo-4-Chloro-3-Indolyl Phosphate/Nitro Blue Tetrazolium (BCIP/NBT): The ALP substrate solution was prepared by diluting a 1% concentration of BCIP (5-bromo-4-chloro-3-indolyl phosphate) to obtain a final dilution of 0.02%

BCIP and 0.03% NBT in 0.1 M Tris-buffered Saline (TBS) with a pH of 9.5. Total 70% Dimethylformamide (DMF) was used to store 1.5% NBT due to its highly volatile nature and to prevent oxidation. To protect the light-sensitive chromogenic substrate, the solution was stored in a brown bottle.

Equal quantities of HAp and rose hip HAp were placed in separate wells or tubes, washed with TBS to eliminate any unbound substances, and subsequently treated with the BCIP/NBT substrate. The samples were then incubated in the dark at room temperature or at 37°C. The presence of ALP activity was indicated by the formation of a blue-purple precipitate on the samples, resulting from the hydrolysis of BCIP by ALP and the subsequent reduction of NBT, which signifies enzymatic activity on the surfaces of HAp and rose hip HAp [25].

ii. AP buffer preparation: The alkaline phosphate buffer was prepared with the following composition and pH: 100 mM Tris-HCl, 100 mM NaCl, 5 mM $MgCl_2$, 0.05% Tween 20, pH 9.5. The components of the buffer were Tris-HCl (MW 157.60) - 15.8 g, NaCl (MW 58.44) - 5.8 g, $MgCl_2$ (MW 203.31) - 1.02 g, and distilled water - 900 mL. All components were mixed to dissolve, and the pH was adjusted to 9.5, bringing the total volume to one liter. Following this, 0.5 mL of Tween 20 solution was added, and the solution was stored at room temperature [26].

iii. ALP activity procedure: The ALP assay was performed to evaluate the enhanced osteogenic differentiation activity of RhHApNPs on the NIH 3T3 cell line (mouse-derived embryonic fibroblasts). NIH 3T3 cells (1×10^5/well) were plated in 96-well plates and incubated at 37°C with 5% CO_2. After the cells reached confluence, 50 mg of untreated cells, HAp, and RhHAp samples were added and incubated for 3, 5, and 7 days, with daily medium changes for both control and treated cells. The sample containing the old media was removed from the well and washed with phosphate-buffered saline (pH 7.4). The cell layers were washed twice with saline and harvested.

The cells were solubilised by the addition of Triton X-100 to a final concentration of 1% and incubated for one minute. Following this, 50 µL of AP buffer was added to all wells. Aliquots of the supernatant were assayed for ALP activity by measuring the cleavage of cells to produce proteins. A 120 µL aliquot of the 5-Bromo-4-chloro-3-indolyl phosphate (BICP)/Nitro Blue Tetrazolium (NBT) working solution was added and incubated for 30 minutes. Cell density was read at 405 nm using an Enzyme-linked Immunosorbent Assay (ELISA) plate reader and visualised using a fluorescence microscope for imaging.

c) Collagen estimation: The Bradford assay was performed for protein estimation [14]. The Bradford method was extensively optimised to estimate the strength of Bradford reagent in the presence of AP buffer. A 100 µL aliquot of each BCIP/NBT (5-Bromo-4-Chloro-3-Indolyl Phosphate/Nitro Blue Tetrazolium) treated sample from the wells was transferred to a fresh 96-well plate. To the 100 µL aliquot of untreated cells (the control group), Normal HAp, and RhHAp, the desired volume of AP buffer and Bradford reagent was added. The volume of Bradford reagent and total reaction volumes in standards and test samples should be the same. Optical Density (OD) was measured for all the supernatants obtained in the wells at 595 nm using an ELISA plate reader. The value of OD was divided by the number of cells counted in each culture as a normalisation criterion. All enzyme activities were expressed as units (micromoles of product formed/min)/g of protein.

STATISTICAL ANALYSIS

The outcomes of the tests were represented graphically using Origin software.

RESULTS

The FESEM analysis revealed nanotubes that were elongated, hexagonal, and spherical in shape. The image also indicated that the material was homogeneous, with larger particles formed by the agglomeration of smaller particles, possibly due to the Van der Waals forces acting between them. It was also found that the majority of the particles ranged between 10-50 nm in size [Table/Fig-2a].

The EDX analysis showed elemental characteristic peaks of Ca, P, O, and C. The peaks of Ca and P were more pronounced, measuring about 25.7 wt% for Ca and 12.9 wt% for P, resulting in a Ca/P wt% ratio of 1.99 [Table/Fig-2b].

X-ray Diffraction (XRD): According to the JCPDS No. 01-1008, the crystallinity of the RhHAp nanoparticles powder is 55.6%. The XRD patterns of the RhHAp are shown in [Table/Fig-2c].

Attenuated Total Reflection - Fourier Transform Infrared Spectroscopy (ATR-FTIR).

The ATR-FTIR analysis shows the peaks of PO_4^{3-} in RhHAp, as demonstrated in [Table/Fig-2d]. The functional groups corresponding to these peaks, as seen in the ATR-FTIR analysis, are given in [Table/Fig-3].

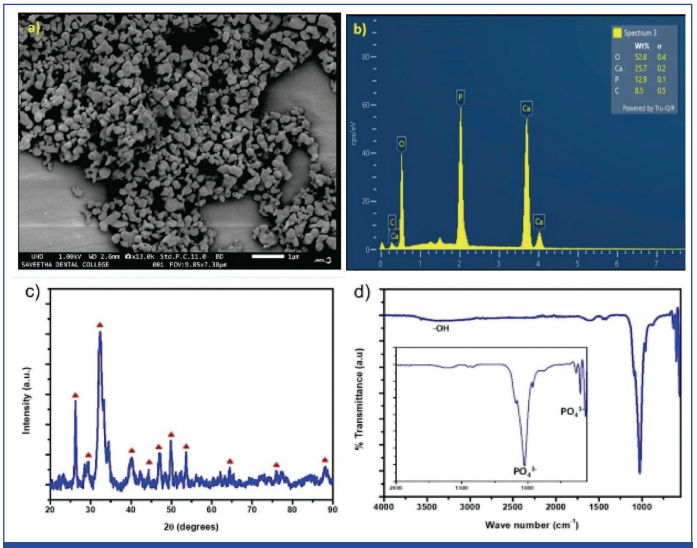

[Table/Fig-2]: a) Scanning Electron Microscopic image of RhHAp, showing agglomeration of smaller HAp particles; b) EDX shows the elemental composition of RhHAp with pea ks of P,Ca, C, and O; c) XRD pattern of RhHAp, where the crystallinity of the material was calculated; d) ATR-FTIR spectrum of RhHAp shows the peaking of PO_4^{3-}

Wave number (cm^{-1})	Functional group
3600-2900	-OH group
1607	C=C aromatic ring and C=C alkenes
1400-1050	Complex υC-O vibrations between phenyl rings
1025	Phosphate
971	γ1 bending mode of phosphate
637	γ4 bending mode of phosphate
591	
575	

[Table/Fig-3]: The functional groups corresponding to the ATR-FTIR analysis readings.

i. Biological characterisation:

a. Blood compatibility: It was observed that limited haemolysis of less than 5% occurred in the set-up, attributed to mechanical injury to the RBCs [Table/Fig-4]. According to the American Society for Testing and Materials standard F756-00, the lysis rate should be below 5% (the critically safe ratio for haemolytic material). Since, the observed RhHAp was under 5%, it can be inferred that it is haemocompatible in nature [23].

II. Chemical characterisation:

a. Calcium mineralisation assay: The ARS assay showed red nodule-like staining across a wide and dense range [Table/Fig-5a]. The staining was denser in nature, indicating more mineralisation

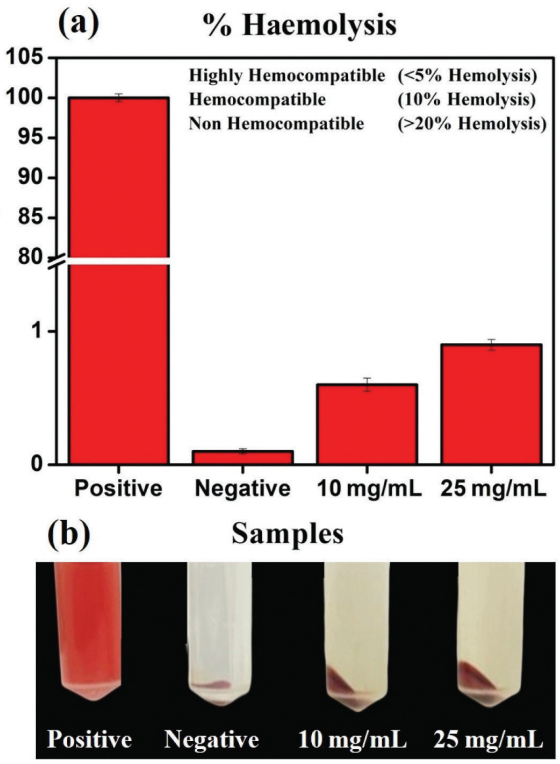

[Table/Fig-4]: a) Haemolytic percentage of the samples namely: Positive Control (PC) - Water, Negative Control (NC) - Saline, 10 µg/mL of RhHAp suspension and 25 mg/mL of RhHAp; and (b) Microcentrifuge tubes showing the photographic images of haemolysis assay on the samples suggesting the highly haemocompatible nature of the nanoparticle.

than the control group. Quantitative analysis was conducted by examining the intensity of the ARS extracted from the stained plates. A microplate reader was employed to determine the OD at the time of staining. The RhHApNPs treated group exhibited a higher OD value than the control HApNPs group. The calcium concentration was 120 µg in the RhHApNPs group, compared to 100 µg for the control group and 20 µg for the untreated cell group [Table/Fig-5b].

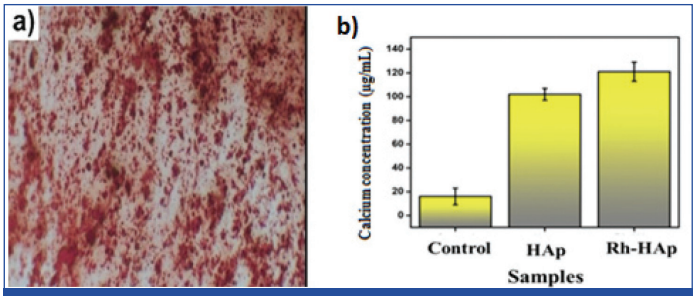

[Table/Fig-5]: a) ARS staining of RhHAp; b) Calcium concentration of control, HAp and RhHAp in osteogenic induction media immediately after staining at 100 µg/mL.

b. Alkaline Phosphatase (ALP) activity: ALP staining was higher in the RhHAp group than in the normal HAp group [Table/Fig-6a]. The RhHAp treated group had higher ALP expression levels of approximately 0.30 µ/mL, compared to 0.275 µ/mL in the normal HAp group and 0.15 µ/mL in the untreated control group [Table/Fig-6b].

c. Collagen estimation: Collagen formation over the hydroxyapatite mesh indicated a positive sign for bone formation. [Table/Fig-7a] shows microscopic imaging of collagen formation in the RhHAp group in the cultured NIH 3T3 cell line. The quantitative assay revealed a significant increase in collagen expression in the RhHApNPs group, measuring approximately 110 µg compared to 90 µg in the HApNPs group and about 40 µg for the untreated control group [Table/Fig-7b].

DISCUSSION

The objective of present study was to formulate Rose hip seed functionalised HApNPs and subject them to physical, chemical,

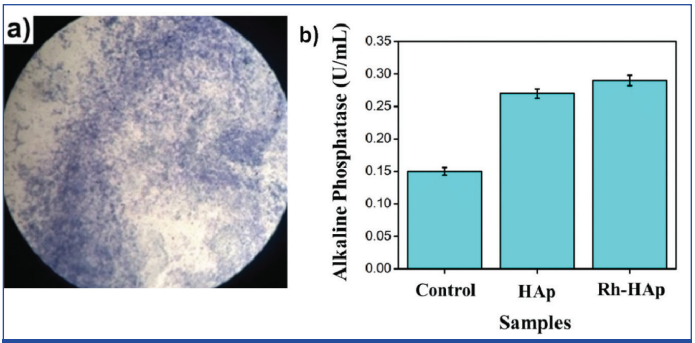

[Table/Fig-6]: a) ALP staining; b) Alkaline phosphatase concentration with control, HAp, and RhHAp in ALP media immediately after staining 100 µg/mL shows increased ALP expression in RhHAp group than the control groups.

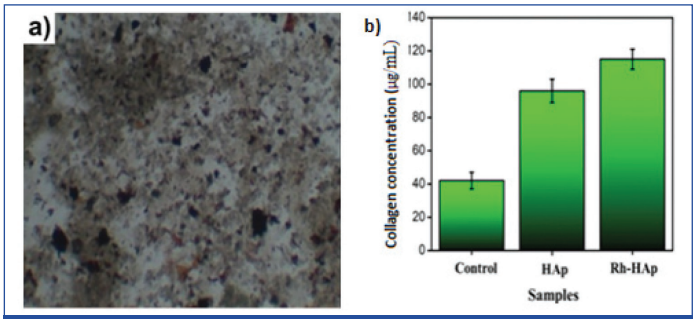

[Table/Fig-7]: a) Microscopic image of the collagen distribution strained; and b) collagen concentration of control, HAp, and RhHAp.

and biological tests using the NIH 3T3 cell line (mouse-derived embryonic fibroblast).

Traditionally, the shape of HApNPs is described as rod-like, spherical, needle-like, or plate-like, with sizes ranging from 5 to 125 nm [27,28]. The observed shapes of RhHApNPs were elongated, hexagonal, and spherical, with a size range of 10 to 50 nm. The alteration in shape could be attributed to the addition of the Rose hip seed extract. Studies on other nanoparticles functionalised with Rose hip extract have also produced spherical-shaped nanoparticles of almost identical size [10]. The EDX analysis coincided with the findings of several other authors in previous studies [29-31]. The obtained ratio of calcium to phosphorus by weight percentage was 1.99, whereas the ideal Ca/P ratio in HAp is 1.67 [32]. Prabakaran K and Rajeswari S reported that a degree of crystallinity ranging between 60% and 70% for biological HAp, with Ca/P ratios of 1.42 and 1.46 respectively, is ideal for medical purposes [33,34].

The ATR-FTIR analysis showed a peak of PO_4^{3-} at 1025 cm^{-1}, along with the presence of other functional groups. Padmanabhan VP et al., also reported similar peak values for the PO group along with the presence of other functional groups in their HApNPs [35].

The HApNPs are generally considered haemolytic as they can cause aggregation of erythrocytes and membrane damage induced by the crystals [36]. The haemolysis test showed a lysis rate of less than 5%, indicating good heamocompatibility of the Rh-HApNPs. The present finding is in concordance with other studies, which reported that nanoporous hydroxyapatite had a similar lysis rate and haemocompatibility [37,38]. The visual assessment was corroborated by the colour of the supernatant. The positive control, which was treated with water, exhibited a deep red hue resulting from the complete lysis of Red Blood Cells (RBCs). In contrast, the test samples retained a light colouration, suggesting minimal haemolytic activity.

The improved mineralisation observed in cells treated with RhHAp nanoparticles, indicated by the intense red staining in the Alizarin Red assay, suggests increased calcium deposition a marker of osteogenic differentiation. The calcium mineralisation assay showed that the RhHApNPs had a higher calcium concentration compared to the control and non RhHApNPs, indicating that the addition of Rose hip seed extract to HAp significantly promotes osteogenic

differentiation. The control group without nanoparticles showed minimal calcium concentration, emphasising the crucial role of HAp-based materials in enhancing mineralisation.

The higher calcium percentage in RhHAp nanoparticles suggests that phytomediated synthesis may enhance both the bioactivity and osteoinductive potential of HAp. Similarly, the ALP expression in the test group was higher than in the control group, indicating that the Rose hip seed extract could reciprocally accelerate ALP activity and its release in the HAp at a higher and earlier rate. A similar elevation in ALP activity has also been noted in several other functionalised variants of HApNPs [39-41].

RhHAp nanoparticles: RhHAp nanoparticles exhibit a superior ability to promote osteogenic differentiation compared to HAp. This enhancement is attributed to the presence of bioactive phytochemicals in the Rose hip extract, such as flavonoids and polyphenols. These compounds are known to possess antioxidant and anti-inflammatory properties that can modulate cellular responses and promote bone regeneration. Specifically, they may enhance osteogenic differentiation by upregulating key osteogenic markers such as ALP, Runt-related transcription factor 2 (Runx2), and osteocalcin, and by activating signaling pathways like Wnt/β-catenin and Bone Morphogenetic Protein (BMP)/Smad. The synergistic effect of these phytochemicals with the hydroxyapatite matrix creates a more favourable microenvironment for osteoblast proliferation and differentiation.

The improved efficacy of RhHAp is likely due to the bioactive phytochemicals found in the Rose hip extract utilised in the synthesis process, which may work in synergy to enhance osteogenic signaling pathways. The Bradford test indicated collagen formation over the hydroxyapatite mesh, which was greater in the RhHApNPs group compared to the control group. The RhHAp exhibited the highest collagen content, indicating enhanced bioactivity. This enhancement could be attributed to the antioxidant and bioactive compounds in the Rose hip seed extract, which may stimulate collagen synthesis and support tissue regeneration. Microscopic imaging supports these findings by showing a denser presence of collagen in treated samples. Collagen (especially type I) constitutes the organic component of natural bone and plays a crucial role in the formation of carbonated apatite material, thus serving as an effective bone marker [42].

Green synthesis of nanoparticles is gaining widespread popularity as it is more economical, feasible, and environmentally friendly, owing to the lack of harmful byproducts [43]. These phytobioactives have emerged as potent elements for hydroxyapatite synthesis due to their high osteogenic potential and biocompatibility [44]. Hydroxyapatite can also be incorporated with various other components, such as CuO and TiO, to enhance osteogenic potential through various techniques [45,46]. Recent studies have revealed that Rose hip extracts are effective substitutes for treating osteoarthritis and bone lesions, showing synergistic antioxidant and chondroprotective activity compared to green tea extract in rat models [47-49]. Rose hip seeds have demonstrated osteogenic potential and a negative effect on the expression of osteoclastic genes when functionalised with magnesium hydroxide nanoparticles. Inherently, this could be due to the presence of flavonoids, along with their antioxidant properties [17]. The present study provides a quantitative evaluation of the synergistic effects brought about by incorporating Rose hip seed extract into hydroxyapatite, thereby enhancing the osteoblastic efficacy of normal hydroxyapatite.

Limitation(s)

A significant limitation of present study was its sole dependence on in-vitro assays. Although the assays performed were beneficial for initial assessments, they do not fully capture the intricate nature of the in vivo bone microenvironment. Key physiological elements, including immune responses, systemic biological interactions, mechanical loading, and long-term degradation processes, are absent from these models, all of which are crucial for understanding the clinical efficacy of biomaterials. To overcome these limitations, future studies should incorporate thorough in vivo investigations utilising suitable small animal models, such as rats or rabbits with critical-sized bone defects, to assess bone regeneration, material integration, and immune responses. Additionally, cytotoxicity estimations should be conducted using assays, including Methyl Thiazolyl Tetrazolium (MTT) live/dead staining, and Lactate Dehydrogenase (LDH) release, to confirm the biocompatibility of RhHAp nanoparticles and ensure safe cellular responses. These measures are essential for progressing RhHAp towards clinical applications in bone tissue engineering.

CONCLUSION(S)

The preparation of RhHApNPs demonstrated significant improvements in physicochemical and biological properties compared to HAp. The synthesised Rh-functionalised HApNPs exhibited elongated, hexagonal, and spherical shapes within the size range of 10-50 nm. An enhanced Ca/P ratio and crystallinity were observed. The functional groups, particularly phosphate groups, indicated the formation of hydroxyapatite. The RhHApNPs exhibited excellent haemocompatibility, with a heamolysis percentage of less than 5%. Furthermore, RhHApNPs significantly promoted osteogenic differentiation, evidenced by increased ALP activity, enhanced calcium deposition, and elevated collagen synthesis, making them a potential candidate for bone tissue engineering.

REFERENCES

[1] Lowe B, Hardy JG, Walsh LJ. Optimizing nanohydroxyapatite nanocomposites for bone tissue engineering. ACS Omega. 2019;5(1):01-09.
[2] Antoniac I, Miculescu F, Cotrut C, Ficai A, Rau JV, Grosu E, et al. Controlling the degradation rate of biodegradable Mg-Zn-Mn alloys for orthopedic applications by electrophoretic deposition of hydroxyapatite coating. Materials. 2020;13(2):263.
[3] Zhang P, Wu H, Wu H, Lu Z, Deng C, Hong Z, et al. RGD-conjugated copolymer incorporated into composite of poly(lactide-co-glycolide) and poly(L-lactide)-grafted nanohydroxyapatite for bone tissue engineering. Biomacromolecules. 2011;12(7):2667-80.
[4] Abdul Halim NA, Hussein MZ, Kandar MK. Nanomaterials-upconverted hydroxyapatite for bone tissue engineering and a platform for drug delivery. Int J Nanomedicine. 2021;16:6477-96.
[5] Munir MU, Salman S, Ihsan A, Elsaman T. Synthesis, characterization, functionalization and bio-applications of hydroxyapatite nanomaterials: An overview. Int J Nanomedicine. 2022;17:1903-25.
[6] Murthy SK. Nanoparticles in modern medicine: State of the art and future challenges. Int J Nanomedicine. 2007;2(2):129-41. PMID: 17722542; PMCID: PMC2673971.
[7] Kozuma W, Kon K, Kawakami S, Bobothike A, Iijima H, Shiota M, et al. Osteoconductive potential of a hydroxyapatite fiber material with magnesium: In vitro and in vivo studies. Dent Mater J. 2019;38(5):771-78. doi: 10.4012/dmj.2018-333.
[8] Irwansyah FS, Noviyanti AR, Eddy DR, Risdiana R. Green template-mediated synthesis of biowaste nano-hydroxyapatite: A systematic literature review. Molecules. 2022;27(17):5586.
[9] Manoj M, Yuan A. A plant-mediated synthesis of nanostructured hydroxyapatite for biomedical applications: A review. RSC Adv. 2020;10(67):40923-39.
[10] Pinho LC, Garbieri TF, Grenho L, Alves MM, Sousa Gomes P, Santos CF, et al. Rosehip extract-functionalized magnesium hydroxide nanoparticles and their effect on osteoblastic and osteoclastic cells. Materials. 2021;14(15):4172.
[11] Husain SE, Sundari SH, Jain RK, Kumar SR. Green synthesis of Terminalia Arjuna-mediated hydroxyapatite nanoparticles: Morphological assessment and evaluation of cytotoxic and antioxidant properties: An in vitro study. J Clin Diagn Res. 2023;17:6-10.
[12] Singh N, Singh V, Singh RK, Pant AB, Pal US, Malkunje LR, et al. Osteogenic potential of Cissus quadrangularis assessed with osteopontin expression. Natl J Maxillofac Surg. 2013;4(1):52-56. Doi: 10.4103/0975-5950.117884. PMID: 24163553; PMCID: PMC3800385.
[13] Zainol Abidin IZ, Johari AN, Yazid MD, Zainal Ariffin Z, Eziwar Dyari HR, Zainal Ariffin SH. Osteogenic potential and bioactive profiles of Piper sarmentosum ethanolic extract-treated stem cells. Pharmaceuticals (Basel). 2023;16(5):708. Doi: 10.3390/ph16050708.
[14] Phetcharat L, Wongsuphasawat K, Winther K. The effectiveness of a standardized rose hip powder, containing seeds and shells of Rosa canina, on cell longevity, skin wrinkles, moisture, and elasticity. Clin Interv Aging. 2015;10:1849-56. Doi: 10.2147/CIA.S90092. PMID: 26604725; PMCID: PMC4655903.
[15] Koczka N, Stefanovits-Bányai É, Ombódi A. Total polyphenol content and antioxidant capacity of rosehips of some Rosa species. Medicines (Basel). 2018;5(3):84. Doi: 10.3390/medicines5030084.

[16] Mármol I, Sánchez-de-Diego C, Jiménez-Moreno N, Ancín-Azpilicueta C, Rodríguez-Yoldi MJ. Therapeutic applications of rose hips from different rosa species. Int J Mol Sci. 2017;18(6):1137.
[17] Kumar GS, Rajendran S, Karthi S, Govindan R, Girija EK, Karunakaran G, et al. Green synthesis and antibacterial activity of hydroxyapatite nanorods for orthopedic applications. MRS Commun. 2017;7(2):183-8. Doi: 10.1557/mrc.2017.48.
[18] Ghate P, Prabhu SD, Murugesan G, Goveas LC, Varadavenkatesan T, Vinayagam R, et al. Synthesis of hydroxyapatite nanoparticles using Acacia falcata leaf extract and study of their anticancerous activity against cancerous mammalian cell lines. Environ Res. 2022;214(Pt 2):113917. Doi: 10.1016/j.envres.2022.113917. Epub 2022 Aug 2. PMID: 35931186.
[19] Prakash M, Rajan HK, Chandraprabha MN, Shetty S, Mukherjee T, Girish Kumar S. Recent developments in green synthesis of hydroxyapatite nanocomposites: Relevance to biomedical and environmental applications. Green Chem Lett Rev. 2024;17(1):2422409. Doi: 10.1080/17518253.2024.2422409.
[20] Jayachandran A, Aswathy TR, Nair AS. Green synthesis and characterization of zinc oxide nanoparticles using Cayratia pedata leaf extract. Biochem Biophys Rep. 2021;26:100995. Doi: 10.1016/j.bbrep.2021.100995. PMID: 33898767; PMCID: PMC8055550.
[21] Spahr DE, Schultz JM. Determination of matrix crystallinity of composites by X-ray diffraction. Polym Compos. 1990;11(4):201-10. Doi: 10.1002/pc.750110402.
[22] Sroka-Bartnicka A, Borkowski L, Ginalska G, Ślósarczyk A, Kazarian SG. Structural transformation of synthetic hydroxyapatite under simulated in vivo conditions studied with ATR-FTIR spectroscopic imaging. Spectrochim Acta A Mol Biomol Spectrosc. 2017;171:155-61. Doi: 10.1016/j.saa.2016.07.032.
[23] Pires AL, de Azevedo Motta L, Dias AM, de Sousa HC, Moraes ÂM, Braga ME. Towards wound dressings with improved properties: Effects of poly(dimethylsiloxane) on chitosan-alginate films loaded with thymol and β-carotene. Mater Sci Eng C Mater Biol Appl. 2018;93:595-605. Doi: 10.1016/j.msec.2018.08.018.
[24] Serguienko A, Wang MY, Myklebost O. Real-time vital mineralization detection and quantification during in vitro osteoblast differentiation. Biol Proced Online. 2018;20:01-05. Doi: 10.1186/s12575-018-0072-y.
[25] Tang Z, Chen H, He H, Ma C. Assays for alkaline phosphatase activity: Progress and prospects. TrAC Trends Anal Chem. 2019;113:32-43. Doi: 10.1016/j.trac.2019.01.024.
[26] Sabokbar A, Millett PJ, Myer B, Rushton N. A rapid, quantitative assay for measuring alkaline phosphatase activity in osteoblastic cells in vitro. Bone Miner. 1994;27(1):57-67. Doi: 10.1016/0169-6009(94)90031-0.
[27] Zhao X, Ng S, Heng BC, Guo J, Ma L, Tan TT, et al. Cytotoxicity of hydroxyapatite nanoparticles is shape and cell dependent. Arch Toxicol. 2013;87(6):1037-52. Doi: 10.1007/s00204-012-0826-0.
[28] Zakharova O, Gusev A, Chuprunov K, Yudin A, Kuznetsov D. Cytotoxic effects of granulated hydroxyapatite with various particle size distribution. IOP Conf Ser Mater Sci Eng. 2020;731(1):012020. Doi: 10.1088/1757-899X/731/1/012020.
[29] Al-Hamdan RS, Almutairi B, Kattan HF, Alresayes S, Abduljabbar T, Vohra F. Assessment of hydroxyapatite nanospheres incorporated dentin adhesive: A SEM/EDX, micro-Raman, microtensile and micro-indentation study. Coatings (Basel). 2020;10(12):1181. Doi: 10.3390/coatings10121181.
[30] Stastna E, Castkova K, Rahel J. Influence of hydroxyapatite nanoparticles and surface plasma treatment on bioactivity of polycaprolactone nanofibers. Polymers (Basel). 2020;12(9):1877. Doi: 10.3390/polym12091877.
[31] Kalaiselvi V, Mathammal R, Vijayakumar S, Vaseeharan B. Microwave-assisted green synthesis of hydroxyapatite nanorods using Moringa oleifera flower extract and its antimicrobial applications. Int J Vet Sci Med. 2018;6(2):286-95. Doi: 10.1016/j.ijvsm.2018.10.002.
[32] Ramesh S, Tan CY, Hamdi M, Sopyan I, Teng WD. The influence of Ca/P ratio on the properties of hydroxyapatite bioceramics. Proc SPIE Int Conf Smart Mater Nanotechnol Eng. 2007;6423:855-60. Doi: 10.1117/12.746112.
[33] Prabakaran K, Rajeswari S. Spectroscopic investigations on the synthesis of nano-hydroxyapatite from calcined eggshell by hydrothermal method using cationic surfactant as template. Spectrochim Acta A Mol Biomol Spectrosc. 2009;74(5):1127-34. Doi: 10.1016/j.saa.2009.09.021. Epub 2009 Sep 19. PMID: 19836296.
[34] Conz MB, Granjeiro JM, Soares GA. Hydroxyapatite crystallinity does not affect the repair of critical-size bone defects. J Appl Oral Sci. 2011;19(4):337-42. Doi: 10.1590/S1678-77572011000400009.
[35] Padmanabhan VP, Kulandaivelu R, Panneer DS, Vivekananthan S, Sagadevan S, Lett JA. Microwave synthesis of hydroxyapatite encumbered with ascorbic acid intended for drug leaching studies. Mater Res Innov. 2020;24(4):207-14. Doi: 10.1080/14328917.2020.1755511.
[36] Elferink JG. Crystal-induced membrane damage: Hydroxyapatite crystal-induced hemolysis of erythrocytes. Biochem Med Metab Biol. 1986;36(1):25-35. Doi: 10.1016/0885-4505(86)90005-4.
[37] Balu S, Sundaradoss MV, Andra S, Jeevanandam J. Facile biogenic fabrication of hydroxyapatite nanorods using cuttlefish bone and their bactericidal and biocompatibility study. Beilstein J Nanotechnol. 2020;11:285-95. Doi: 10.3762/bjnano.11.22.
[38] Palanivelu R, Kumar AR. Synthesis, characterization, in vitro anti-proliferative and hemolytic activity of hydroxyapatite. Spectrochim Acta A Mol Biomol Spectrosc. 2014;127:434-8. Doi: 10.1016/j.saa.2014.01.059.
[39] Haniastuti T, Susilowati H, Rinastiti M. Viability and alkaline phosphatase activity of human dental pulp cells after exposure to yellowfin tuna bone-derived hydroxyapatite in vitro. Int J Dent. 2020;2020:8857534. Doi: 10.1155/2020/8857534.
[40] Wang Z, Han T, Zhu H, Tang J, Guo Y, Jin Y, et al. Potential osteoinductive effects of hydroxyapatite nanoparticles on mesenchymal stem cells by endothelial cell interaction. Nanoscale Res Lett. 2021;16(1):67. Doi: 10.1186/s11671-021-03525-4.
[41] Malysheva K, Kwaniak K, Gnilitskyi I, Barylyak A, Zinchenko V, Fahmi A, et al. Functionalization of polycaprolactone electrospun osteoplastic scaffolds with fluorapatite and hydroxyapatite nanoparticles: Biocompatibility comparison of human versus mouse mesenchymal stem cells. Materials (Basel). 2021;14(6):1333. Doi: 10.3390/ma14061333.
[42] Wang Y, Azaïs T, Robin M, Vallée A, Catania C, Legriel P, et al. The predominant role of collagen in the nucleation, growth, structure and orientation of bone apatite. Nat Mater. 2012;11(8):724-33. Doi: 10.1038/nmat3362.
[43] Singh H, Desimone MF, Pandya S, Jasani S, George N, Adnan M, et al. Revisiting the green synthesis of nanoparticles: Uncovering influences of plant extracts as reducing agents for enhanced synthesis efficiency and its biomedical applications. Int J Nanomedicine. 2023;18:4727-50. Doi: 10.2147/IJN.S412593.
[44] Gupta A, Mehta SK, Qayoom I, Gupta S, Singh S, Kumar A. Biofunctionalization with Cissus quadrangularis phytobioactives accentuates nano-hydroxyapatite-based ceramic nano-cement for neo-bone formation in critical-sized bone defect. Int J Pharm. 2023;642:123110. Doi: 10.1016/j.ijpharm.2023.123110.
[45] Preetha PM, Radha G, Arul KT, Ramya JR. Enhanced biocompatibility and antibacterial efficacy of CuO-HAp nanocomposite for hard tissue regeneration and repair. Inorg Chem Commun. 2025;171:113654. Doi: 10.1016/j.inoche.2024.113654.
[46] Wang Q, Yusoff M, Khairuddin NAACM, Roslan NA, Razali MH. Antibacterial TiO_2 nanoparticles and hydroxyapatite loaded carboxymethyl cellulose bio-nanocomposite scaffold for wound dressing application. Materials Chemistry and Physics. 2025;340:130835.
[47] Jeong C, Bae D, Lim H, Lee M, Kang N, Kim S. Ameliorative effects of green tea seed extract with rose hip powder (Rosa canina L.) on regulation of pain and inflammatory cytokines in a rat model of monosodium iodoacetate-induced experimental osteoarthritis. Anim Cells Syst (Seoul). 2015;19(1):69-77. Doi: 10.1080/19768354.2015.1006021.
[48] Schwager J, Richard N, Schoop R, Wolfram S. A novel rose hip preparation with enhanced anti-inflammatory and chondroprotective effects. Mediators Inflamm. 2014;2014:105710. Doi: 10.1155/2014/105710.
[49] Larsen E, Kharazmi A, Christensen LP, Christensen SB. An anti-inflammatory galactolipid from rose hip (Rosa canina) that inhibits chemotaxis of human peripheral blood neutrophils in vitro. J Nat Prod. 2003;66(7):994-5. Doi: 10.1021/np0300128.

PARTICULARS OF CONTRIBUTORS:
1. Fellow in Cleft Orthodontics, Department of Orthodontics, Meenakshi Ammal Dental College and Hospital, Meenakshi Academy of Higher Education and Research (Deemed to be University), Chennai, Tamil Nadu, India.
2. Professor, Department of Orthodontics, Meenakshi Ammal Dental College and Hospital, Meenakshi Academy of Higher Education and Research (Deemed to be University), Chennai, Tamil Nadu, India.
3. Assistant Professor, Department of Orthodontics, Meenakshi Ammal Dental College and Hospital, Meenakshi Academy of Higher Education and Research (Deemed to be University), Chennai, Tamil Nadu, India.

NAME, ADDRESS, E-MAIL ID OF THE CORRESPONDING AUTHOR:
Dr. Ratna Parameswaran,
Professor, Department of Orthodontics, Meenakshi Ammal Dental College and Hospital, Meenakshi Academy of Higher Education and Research (Deemed to be University), Chennai-600095, Tamil Nadu, India.
Email: drratna.ortho@madch.edu.in

PLAGIARISM CHECKING METHODS: [Jain H et al.]
- Plagiarism X-checker: Jan 30, 2025
- Manual Googling: Jul 11, 2025
- iThenticate Software: Jul 14, 2025 (7%)

DENTISTRY: Author Origin

EMENDATIONS: 8

AUTHOR DECLARATION:
- Financial or Other Competing Interests: None
- Was Ethics Committee Approval obtained for this study? Yes
- Was informed consent obtained from the subjects involved in the study? Yes
- For any images presented appropriate consent has been obtained from the subjects. NA

Date of Submission: **Jan 28, 2025**
Date of Peer Review: **Mar 23, 2025**
Date of Acceptance: **Jul 17, 2025**
Date of Publishing: **Apr 01, 2026**